====== **GEOPHYSICS** ======

Hydrodynamic Spirality in Geodynamo Models

M. Yu. Reshetnyak[a] and B. Steffen[b]

Presented by Academician G.S. Golitsyn November 10, 2005

Received November 11, 2005

Generation of geomagnetic field is related to dynamo processes in the earth's liquid core. It is one of the basic problems of geophysics. The geomagnetic field can be generated by both large-scale [1] and small-scale [2] flows. The latter possibility is closely related to the α-effect concept of the theory of intermediate fields [3]. The nature of the α-effect consists in the reflection symmetry distortion in a convective rotating body, as a result of which the number of rightward rotating whirls in the Northern Hemisphere, for example, is systematically greater than the number of leftward rotating whirls. And vice versa, the leftward rotating whirls prevail over the rightward rotating ones in the Southern Hemisphere. The reflection symmetry distortion due to Maxwell's equations smoothing in turbulent pulsations produces the intermediate magnetic field component **B** parallel to the average electric current $\mathbf{J} = \alpha\mathbf{B}$. The distortion of the reflective invariance in the rotating turbulence is usually attributed to the influence of Coriolis forces upon the whirls traveling in a non-zero density gradient body (see, for example, [4]). Let the body density decrease with radius. Then, the rising whirl expands and a whirl radius-oriented velocity appears. Consequently, the Coriolis force induced by the radial velocity and general rotation is generated. This force twists the whirl in the direction opposite to the general rotation. Similarly, a descending whirl contracts and a radial velocity appears therein. Therefore, the Coriolis force twists this whirl in the direction concurrent with the general rotation. Consequently, we obtain a non-zero correlation:

$$\chi^H = \langle \mathbf{v} \cdot \mathrm{rot}\,\mathbf{v} \rangle, \tag{1}$$

i.e., the average flow spirality (here **v** is the turbulent velocity and $\langle \ldots \rangle$ is the averaging symbol). Correlation (1) determines the α-effect magnitude (Moffat's formula):

---
[a] *Schmidt Institute of Physics of the Earth,*
   Russian Academy of Sciences, ul. Bol'shaya Gruzinskaya 10,
   Moscow, 123995 Russia
[b] *Julich Research Center, Julich, Germany*

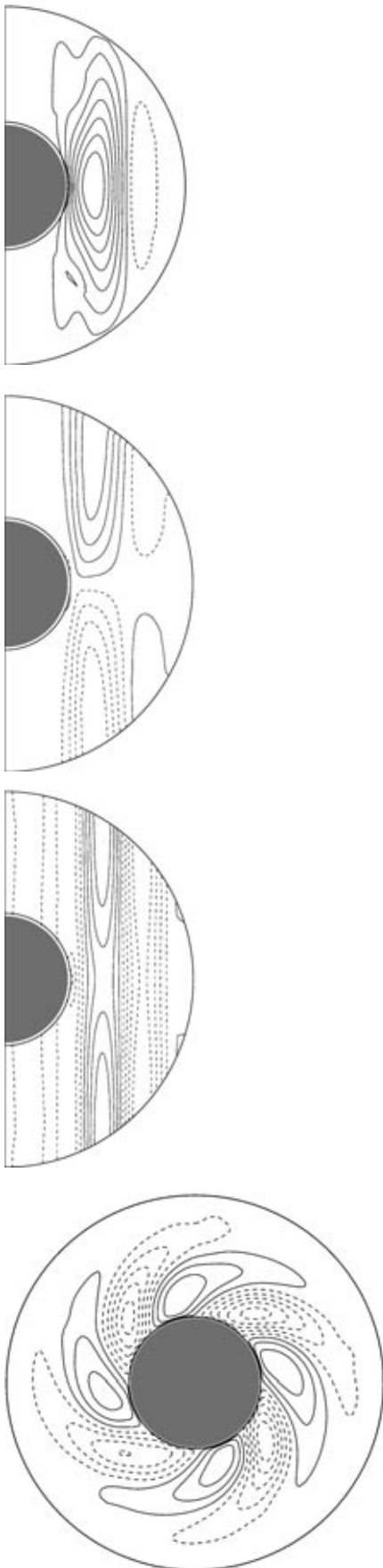$$\alpha = -\frac{\tau^H \chi^H}{3}, \tag{2}$$

where τ^H is the characteristic correlation time. However, this conventional α-effect explanation has a limited implication. First, it is not always possible in applied problems to separate the averaged flow $\overline{\mathbf{V}}$ and the turbulent (stochastic) component **v** required in the theory of intermediate fields [3]. Relation (2) between the spirality and the α-effect has such a simple form only in the case of a local homogeneous and isotropic turbulence. Finally, the medium of magnetic field generation is far from being always compressible. Therefore, the notion of expanding and contracting whirls has limited implication. The noted limitations are especially characteristic for two essential dynamo instances (planetary and laboratory). In laboratory simulations, liquid sodium used as the working medium can be considered absolutely uncompressible. The density of the earth's outer core, related to the geodynamo mechanism action and mainly composed of liquid iron, varies along the radius within a narrow range of 15–20% [5], while the medium compressibility due to temperature fluctuations is negligible.

At the same time, it is well known that even the initial 3D geodynamo models with the Boussinesq approximation [6] yielded regimes with non-zero large-scale spirality. Further, we consider mechanisms of spirality generation in such systems and compare the obtained results with the known solar dynamo models [7, 8].

Let us consider thermal convection equations for an uncompressible liquid ($\nabla \cdot \mathbf{V} = 0$) in a spherical layer ($r_i \leq r \leq r_0$) rotating around axis z with the angular velocity Ω, where r, θ, φ is the spherical system of coordinates. Having adopted the following units of measurement for velocity **V**, time t, and pressure P: $\frac{\kappa}{L}$, $\frac{L^2}{\kappa}$,

and $\frac{\rho\kappa^2}{L^2}$, where L is the unit of distance, κ is the coef-

ficient of molecular thermal conductivity, and ρ is the density of substance, we obtain:

$$E \cdot Pr^{-1}\left[\frac{\partial \mathbf{V}}{\partial t} + (\mathbf{V} \cdot \nabla)\mathbf{V}\right]$$

$$= \mathrm{rot}\mathbf{B} \times \mathbf{B} - \nabla P - \mathbf{1}_z \times \mathbf{V} + RaTr\mathbf{1}_r + E\Delta\mathbf{V}, \quad (3)$$

$$\frac{\partial T}{\partial t} + (\mathbf{V} \cdot \nabla)(T + T_0) = \Delta T.$$

The nondimensional Prandtl, Eckman, and Rayleigh numbers are set in the following forms: $Pr = \dfrac{\nu}{\kappa}$, $E = \dfrac{\nu}{2\Omega L^2}$, and $Ra = \dfrac{\alpha g_0 \delta T L}{2\Omega\kappa}$, where ν is the coefficient of kinematic viscosity; α is the coefficient of volume expansion ratio; g_0 is the acceleration of gravity; and δT is the unit of temperature T disturbance relative to the equilibrium profile $T_0 = \dfrac{r_i/r - 1}{1 - r_i}$, $r_0 = 1$. Let us introduce the Rossby number as $Ro = E \cdot Pr^{-1}$. Problem (3) is confined by the boundary conditions on $r = r_i, r_0$. For the temperature T disturbances, zero boundary conditions are applied. In order to prevent any further spirality generation in the thin Eckman layer, the nonpenetration condition $V_r = 0$ and a nonviscous stress condition for the tangential velocity components V_θ and V_φ are adopted for the velocity field. The numerical procedures are described in [9].

Increase in the Rayleigh number Ra will provoke a convective instability in the form of vertical columns with the diameter $\sim E^{1/3}$. Therefore, modeling with the earth's realistic Eckman number $E \sim 10^{-15}$ requires the application of special turbulence models [11]. Figure 1 presents typical sections of velocity components showing the appearance of vertical columns at $Ra = 100$, $Ra^{cr} \sim 13$. Further increase in the Rayleigh number provokes not only downscaling (Fig. 2) but also the appearance of a large-scale velocity component with wave numbers $n < n^{cr}$, which is quite prominent in the additional spectral analysis. However, like in the previous case, the φ spectrum maximum corresponds to the diameter of columns at the agitation threshold. In the absence of superviscosity (i.e., when the turbulent viscosity factor is a function of n, as $\nu_T \sim \nu_0(1 + cn^3)$), the existence of the maximum in the kinematic energy spectrum is quite prominent in a number of dynamo

Fig. 1. For $E = 10^{-4}$, $Pr = 1$, $Ra = 10^2$ (from top to bottom): meridional section of the nonaxisymmetric term of the velocity components V_r-, V_θ-, and V_φ (–4.0, 16.9), (–28.2, 28.4), (–33.6, 38.6). The bottom figure is the equatorial section of the nonaxisymmetric term V_r of the velocity field component (–23.9, 17.3). Values in parentheses correspond to the component variation range.

models for both small Ra ~ 10 Ra^{cr} and developed convection with Ra ~ 10^2 Ra^{cr} [13]. The two considered regimes are characterized by separation of the liquid core into two domains: domain I over (beneath) the solid core confined by the Taylor cylinder and domain II beyond the Taylor cylinder. If convection appears in the external domain II and is virtually absent in domain I at the generation threshold Ra = Ra^{cr} and moderate Rayleigh numbers (Fig. 1), then the convection intensity maximum will shift toward domain II with magnification of the amplitude of thermal sources (Fig. 2). However, the domains are quite prominent in both instances considered. As it has been mentioned above, spirality is generated in uncompressible liquid models [6], where the viscous boundary conditions $\mathbf{V} = 0$ were used. Figure 3 shows averaged (in time and azimuth coordinate φ) hydrodynamic spirality χ^H distribution for the above two generation regimes (I and II). Below, we consider physical mechanisms of χ^H generation at $\nabla \cdot \mathbf{V} = 0$.

In general, the development of spirality models is based on the computation of a pseudo-scalar value obtained from the scalar product of two vectors: the ordinary vector $\mathbf{G}$ and the axial vector $\mathbf{w}$. For the Parker model [4] considered above, $\mathbf{G}$ corresponds to the large-scale density gradient of the medium, and $\mathbf{\Omega}$ is used as the second vector. However, although the Parker model was initially developed precisely for the solar dynamo, the subsequent helioseismologic observations imposed extra limitations on the spirality χ^H distribution in the convection zone of the sun: the sign of spirality must change along the radius, which obviously does not agree with the assumption that $\dfrac{\partial \rho}{\partial r} < 0$

in the entire convection zone. According to the alternative scenario of the origination of spirality and α-effect suggested in [7, 8], the α-effect in the lower domain of the convective zone is subject not to the density gradient, but to the kinetic energy gradient ∇E_K. This mechanism is interesting at least due to the much more frequent manifestation of the spatial heterogeneity of kinematic energy relative to the spatial heterogeneity of density. The above concepts of the generation of large-scale magnetic fields by a small-scale turbulence in the uncompressible liquid do not contradict the known geodynamo calculations [6]. In order to illustrate this statement, let us consider the linear-regime χ^H generation by
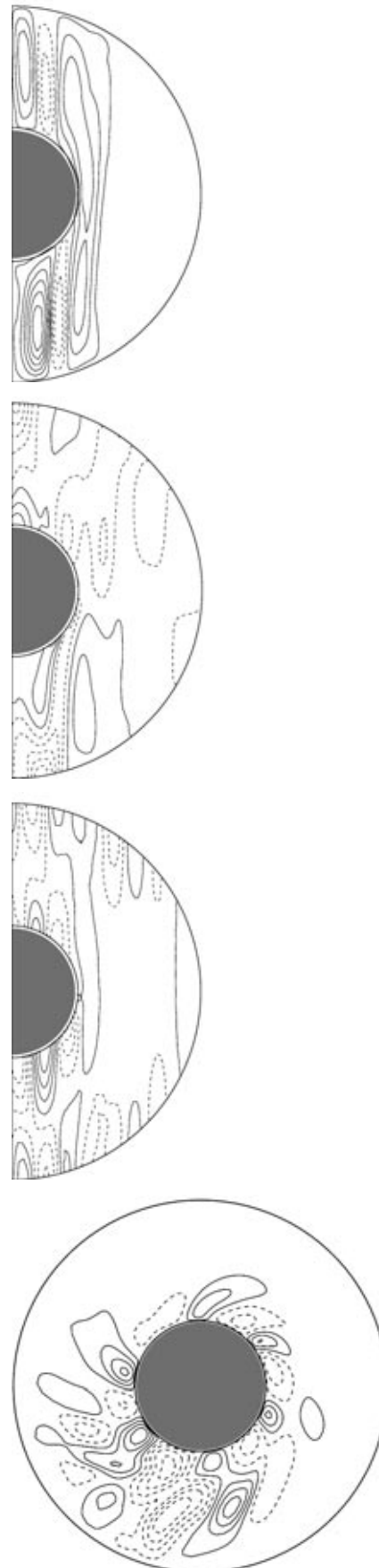

Fig. 2. For E = 10^{-4}, Pr = 1, Ra = $5 \cdot 10^2$ (from top to bottom): meridional section of the nonaxisymmetric term of the velocity components V_r-, V_θ-, and V_φ (–46.5, 104.6), (–111.1, 72.1), (–132.4, 136.8). The bottom figure is the equatorial section of the nonaxisymmetric term V_r of the velocity field component (–129.6, 128.0).
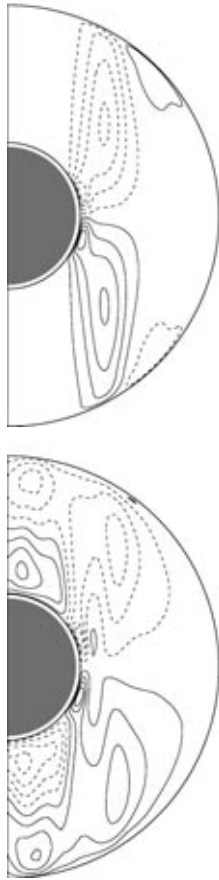
$$\chi^{H} \;=\; v_z^* w_z \;=\; \frac{ik_z}{\mathrm{E}(\mathrm{Pr}^{-1}\omega + k^2)}|v_z|^2,$$

where $\omega = -i\dfrac{\partial}{\partial t}\,\mathbf{v}/\mathbf{v}$ is the imaginary part of the growth velocity. Then,

$$\Re\chi^{H} \;=\; \frac{2\mathrm{Pr}\,\omega k_z}{\mathrm{E}(\omega^2 + |k|^4\mathrm{Pr}^2)}.$$

According to the dispersion analysis [11], two solutions with $\pm k$ (waves traveling in the opposite directions) are implemented for the defined ω. Therefore, generation of spirality can possess both positive (at $k_z > 0$) and negative (at $k_z < 0$) values. The total spirality turns out to be equal to zero, like in the case of Alven waves in an unlimited space. Therefore, more subtle effects should be taken into consideration.

The emergence of non-zero spirality χ^{H} turns out to be related to two effects: Eckman layers and the layer boundary inclination that provokes variation of the column height. In the first case, the Eckman layer boundary is marked by the appearance of the non-zero normal velocity component $\sim\!\mathrm{E}^{1/2}$ that generates the spirality ($\sim\!\mathrm{E}^{1/2}$). In the Northern Hemisphere, the spirality is positive at the outer boundary of the core and negative at the solid core boundary. The spatial scale of spirality in the normal direction to the boundary corresponds to the Eckman layer thickness $\delta_{\mathrm{E}} \sim \mathrm{E}^{1/2}$. This case is not interesting for geodynamo. Due to the nonviscous boundary conditions for $\mathbf{V}$, such a possibility is excluded in our calculations (Figs. 1, 2). The second case is more interesting. By applying expansion along the column height, which depends on the distance s of column from the rotation axis s, it was demonstrated that the sign of spirality will alternate with increase (decrease) in the column height. This effect is related to Rossby waves, which induce s variations and the consequent additional torsion provoked by the dislocation. This effect was usually considered for the external part of core II, where decrease in s increases the column height. We believe that precisely this phenomenon is responsible for the appearance of spirality $\chi^{H} < 0$ in both [15] and our calculations (Fig. 3) for small Ra values.

In the case of large Ra values (typical of geodynamo), the "tubular" mechanism of heat transfer in domain II turns out to be insufficient, and convection shifts toward domain I where motions induced by buoyancy forces are parallel to the rotation axis, whereas the heat motion and transfer from the higher-temperature solid core to the external boundary is less impeded by the Coriolis force. In this case, in the Northern Hemisphere, increase of s at the boundary with the solid core increases the column height, resulting in the appearance of $\chi^{H} > 0$ [14]. Consequently, at large Ra values, χ^{H} is confined to the Taylor cylinder and is sign-variable (Fig. 3). In this case, each column will have an

Fig. 3. A meridional section of the axisymmetric spirality term χ^{H} (from top to bottom): Ra $= 10^2$ $(-6.9 \cdot 10^5, 6.9 \cdot 10^5)$, Ra $= 5 \cdot 10^2$ $(-3.1 \cdot 10^7, 3.0 \cdot 10^7)$.

the Coriolis force in a flat layer at $\mathbf{1}_{\boldsymbol{\Omega}} = \mathbf{1}_z$. From $\dfrac{\partial \mathbf{V}}{\partial t} \sim$ $-\mathrm{Ro}^{-1}\mathbf{1}_z \times \mathbf{V}$, it follows that

$$\frac{\partial}{\partial t}(\mathbf{V}\cdot\mathrm{rot}\,\mathbf{V}) \sim \mathrm{Ro}^{-1}\!\left(\frac{\partial E_k}{\partial z} - V_z\mathrm{div}\,\mathbf{V} + [\mathrm{rot}\,\mathbf{V}\times\mathbf{V}]_z\right)\!.(4)$$

The Parker model took into consideration the second term. This is characteristic of gaseous bodies with high-density gradients and the homogeneous distribution of kinetic energy. Obviously, in a planetary dynamo, where the magnetic field appears in a low-compressible medium, the role of the first term can be very high. Regarding the third term in (4), a more detailed analysis of the shape of originating flows shows that the maximum input in spirality corresponds to the product $\mathrm{rot}_z\mathbf{v}\cdot v_z$. Correspondingly, the third term in the principal order is equal to zero. The next necessary condition for the appearance of a large-scale spirality is as follows: correlation of phases v_z and w_z is equal to $\mathrm{rot}_z\mathbf{v}$. It can be demonstrated that, in k-space at the agitation threshold for the neutral mode, we will have

invariable sign for v_z, whereas the sign of w_z will be height-variable.

Spirality generation mechanisms considered above can exist in the earth's liquid core along with the conventional Parker mechanism [4]. Acting simultaneously, these mechanisms increase spirality near the external boundary and attenuate one another near the solid core due to the opposite-phase action. Inasmuch as the spirality is asymmetric relative to the equatorial plane in both mechanisms, the total spirality will also possess this feature.

ACKNOWLEDGMENTS

REFERENCES

1. E. C. Bullard and H. Gellman, Phil. Trans. R. Soc. Lond. **A247**, 213 (1954)
2. S. I. Wainstein, *Magnetic Fields in the Space* (Nauka, Moscow, 1983) [in Russian]
3. F. Krause and K. H. Rädler, *Mean Field Magnetohydrodynamics and Dynamo Theory* (Akademie Verlag, Berlin, 1980).
4. E. N. Parker, *Cosmical Magnetic Fields* (Oxford University Press, Oxford, 1979; Mir, Moscow, 1982)
5. *Geomagnetism*, Ed. by J. A. Jacobs (Academic Press, New York, 1988)
6. G. A. Glatzmaier and P. H. Roberts, Phys. Earth Planet. Inter. **91**, 63 (1995)
7. V. I. Krivodubskii, Astronom. Zh. **61**, 540 (1984)
8. R. Rüdiger and L. L. Kitchatinov, Astron. Astrophys. **269**, 581 (1993)
9. M. Reshetnyak and B. Steffen, Numer. Methods Program. **6**, 27 (2005). http://www.srcc.mcu.su/num-meth/english/index.html.
10. B. M. Boubnov and G. S. Golitsyn *Convection in Rotating Fluids* (Kluwer Acad. Publ., London, 1995)
11. M. Yu. Reshetnyak, Dokl. Akad. Nauk. **400**, 105 (2005) [Dokl. Earth Sci. **400**, 279 (2005)].
12. C. Kutzner and U. R. Cristensen, Phys. Earth. Planet. Inter. **131**, 29 (2002)
13. P. H. Roberts and G. A. Glatzmaier, Phil. Trans. R. Soc. Lond. **358**, 1109 (2000)
14. F. H. Busse, Phys. Earth. Planet. Inter. **12**, 350 (1976)
15. A. Kageyama and T. Sato, Phys. Plasmas **4**, 1569 (1997).